Available online at www.sciencedirect.com

SciVerse ScienceDirect

journal homepage: www.elsevier.com/locate/he

Hydrogen from acetic acid as the model compound of biomass fast-pyralysis oil over Ni catalyst supported on ceria–zirconia

Xiao-xiao Zheng, Chang-feng Yan, Rong-rong Hu, Juan Li, Hang Hai, Wei-min Luo, Chang-qing Guo, Wen-bo Li, Zhou-yu Zhou*

Guangzhou Institute of Energy Conversion, Chinese Academy of Sciences, Guangzhou 510640, China

ARTICLE INFO

Article history:
Received 16 December 2011
Received in revised form
8 May 2012
Accepted 15 May 2012
Available online 18 June 2012

Keywords:
Bio-oil
Model compound
Acetic acid
Hydrogen
Ni catalyst supported on ceria–zirconia

ABSTRACT

Hydrogen production from catalytic steam reforming of model compound acetic acid of bio-oil was investigated under atmospheric pressure in a bench-scale fixed-bed reactor and a series of Ni catalysts supported on ceria–zirconia were prepared via co-precipitation with varying contents of Ni and Ce loading. Simultaneously, effects of reaction temperature, and molar ratio of steam to carbon fed, liquid hourly space velocity (LHSV) were also explored. The results indicated that the 12Ni/7.5Ce-Zr-O catalyst was superior to other catalysts with different Ni and Ce loading. At $T = 650$ °C, $S/C = 3$, LHSV $= 2.8$ h^{-1}, the reaction over Ni catalyst supported on ceria–zirconia turns out that the highest activity and the maximum hydrogen selectivity of 83.4% and the minimum methane selectivity of 0.39% are attained. Besides, Ni catalyst supported on ceria–zirconia shows good stability during 25 h continuous reaction without any deactivation.

1. Introduction

Hydrogen production is one of the most important technologies for the chemical industry, power generation and fuel cell applications [1]. Hydrogen as a second energy can be produced from a variety of resources. The traditional methods for producing hydrogen are catalytic steam reforming of natural gas and oil-derived naphtha, and partial oxidation of heavy oils [2]. Though these technologies are mature enough into market value, the fossil fuels have been heavily consumed with a large quantity of CO_2 being released [3]. Therefore, some new feedstock related to be environmentally friendly should be found, such as biomass, which is renewable and with no contribution to a net increase in atmospheric carbon dioxide.

The main method available for the hydrogen production from biomass is thermo chemical conversion of biomass to hydrogen, including steam gasification [4,5] high-pressure supercritical conversion [6,7] and steam-reforming of bio-oils [2,8–13]. Bio-oil is a liquid by fast pyrolysis of biomass, composed by a complex mixture of oxygenated organic molecules and water. Due to its ease of storage and transport, as well as higher energetic density, hydrogen production by steam reforming of bio-oil is recognized as one of the most promising and economical ways to producing hydrogen.

Up to now, numerous researches have been done on the steam reforming of the biomass pyrolysis oil, and the majority focus on the developing of high activity, high selectivity and high stability of reforming catalyst which easily deactivated

* *Corresponding author*. Tel./fax: +86 02087057729.
E-mail address: yancf@ms.giec.ac.cn (C.-f. Yan).

0360-3199/$ – see front matter
doi:10.1016/j.ijhydene.2012.05.067

by the deposit of carbon [14,15]. Because of the complicated organic components in bio-oil, at the preliminary test, some model oxygenate components are used for designing the efficient catalysts [8–11,14,19]. Acetic acid is one of the major components and usually investigated with various supported metal catalysts as the model compound of bio-oil [11,15–18]. Basagiannis [17] has taken acetic acid as the model compound and tested a variety of metals, such as Pt, Pd, Rh and Ni, loaded on the various carriers such as Al_2O_3, La_2O_3/Al_2O_3, MgO/Al_2O_3 and CeO_2/Al_2O_3. The results showed that Ni-based and Ru-based catalysts presented high activity and high selectivity toward hydrogen. The order of catalytic activity was 17% Ni/Al_2O_3 > 0.5% Rh/Al_2O_3 > 1% Ru/Al_2O_3 > 1% Pd/Al_2O_3 > 1% Pt/Al_2O_3. Besides, Basagiannis [18] in the other article also proved that with Ni presenting catalytic activity was shifted toward lower temperatures and nickel promoted steam reforming reactions and retards the rate of carbon deposition onto the catalyst surface. Cyrille [19] has investigated the steam reforming of the bio-oil model compounds over Pt, Pd and Rh supported on alumina and a ceria–zirconia sample. As a result, the ceria–zircionia materials showed a higher activity than the corresponding alumina samples. The order of catalytic activity was 1% Rh–$CeZrO_2$ > 1% Pt–$CeZrO_2$ ~ 1% Rh–Al_2O_3 > 1% Pd–$CeZrO_2$ > 1% Pt–Al_2O_3 > 1% Pd–Al_2O_3. The steam reforming of acetic acid as well as water gas shift reaction occurs simultaneously and the overall process can be described as $C_2H_4O_2 + H_2O \rightarrow 2CO_2 + 4H_2$. In addition to the reforming reaction, many side effects take place as well such as thermal decomposition ($C_2H_4O_2 \rightarrow$ gas (CO, CO_2, H_2, CH_4, C_2H_4, C_2H_6…) + coke), ketonization ($2C_2H_4O_2 \rightarrow C_3H_6O + CO_2 + H_2O$), methanation ($CO_2 + 4H_2 \rightarrow CH_4 + 2H_2O$, $CO+3H_2 \rightarrow CH_4+H_2O$), and boudouard reaction ($C + CO_2 \rightarrow 2CO$) [20,21]. Methane as one of the by-products occupies more hydrogen atom, so the catalyst which promotes reforming of methane to product hydrogen is also right useful for reforming of acetic acid. Roh [22]has loaded Ni on to different carriers ZrO_2, CeO_2, $MgAl_2O_4$, Ce–ZrO_2, which were evaluated by the steam reforming of methane. Finally, Ni/Ce–ZrO_2 showed the highest activity (97% CH_4 conversion) as well as high stability and the H_2 concentration in the reactor effluent was 62%. The values of CH_4 conversion and H_2 concentration reached very close to their own equilibrium values (CH_4 conversion: 99.4% and H_2 concentration: 62.7%). Besides, catalyst Ni/Ce–ZrO_2 also showed a good activity in steam reforming of ethanol for production of hydrogen [23–25].

In the previous work, certain results had been obtained in our group by steam reforming of bio-oil aqueous fraction over Ni/CeO_2–ZrO_2 catalyst. The results showed that hydrogen yield depends on the Ni and Ce loading weight, the reaction temperature and the ratio of water to bio-oil. And under the same condition, the effect of Ni/CeO_2–ZrO_2 catalyst is superior to the commercial nickel-based catalyst Z417 [26]. In order to further investigate the performance of Ni catalyst supported on ceria–zirconia, we choose acetic acid as our model compound of bio-oil. In the paper, a series of Ni catalysts supported on ceria–zirconias with different Ni and Ce loaded weight; the effect of the reaction temperature, steam to carbon ratio, liquid hourly space velocity (LHSV) and the stability of Ni catalyst supported on ceria–zirconia were evaluated.

2. Experiments

2.1. Catalysts preparation

The ZrO_2 support and the promoter CeO_2 were prepared by the co-precipitation method. The aqueous solution of $ZrOCl_2$ and Ce $(NO_3)_3 \cdot 6H_2O$ with different Ce^{4+} concentration were added to vigorously stirred solution of NH_4OH according to the ratios of n (Zr)/n (OH^-) and n (Ce)/n (OH^-) at $T = 50$ °C, pH = 9. The resulted precipitates were filtered and washed with distilled water, then dried in air at 110 °C for 6 h. Finally, the mixed oxide precursors were calcined in air at 600 °C for 6 h.

A series of Ni catalyst supported on ceria–zirconias were prepared by the initial wet impregnation method, which described in detail elsewhere [18]. The solid residue was drying at 110 °C for 12 h, followed by calcinating at 800 °C for 6 h and naturally cooling for testing. The specific metal loadings for Ni were 0%, 2.5%, 5%, 7.5%, 10%, 12% and for Ce were 0%, 2.5%, 5%, 7.5%, and 10%.

The catalytic materials are referred to as xNi/yCe-Zr-O (where x, y are the Ni and Ce metal wt% respectively) for samples supported on ceria–zirconias solid solution.

2.2. Catalyst characterization

Specific surface areas of supports and catalysts were measured with the BET technique using a Micromeritics ASAP-2010 apparatus, employing nitrogen as the absorbent at 77 K. Prior to each measurement, the sample was outgassed to eliminate volatile adsorbents on the surface at 250 °C for 4 h.

X-ray diffraction (XRD) patterns of supports and catalysts were obtained on a Philips D/MAX-IIIA powder diffractometer, with a Cu Kα radiation (0.154 nm). Scans were collected in the range of 15–75° at a scanning rate of 5°/min at 40 mA and 40 kV.

2.3. Experimental system

The experiments of the catalytic steam reforming of acetic acid were carried out in a bench-scale fixed-bed placed in a tubular quartz reactor which filled with about 3 g catalyst powder and 26 g ceramic column and ball as the preheater upon the catalyst under atmospheric pressure. The calcined catalyst was reduced in situ in 5% H_2/N_2 stream at 700 °C for 4 h prior to reaction. The schematic flow diagram of the experimental system is shown in Fig. 1. The temperature ($T = 500$–900 °C) was controlled by one thermocouple placed inside the reactor directly measuring the temperature of the bed. The liquid (S/C = 0, 1.5, 2, 2.5, 3, 3.5) was fed in by a syringe pump at a certain speed, and then converted into vapor by the high temperature ceramic before it reached the catalyst. The carrier gas N_2 flow rate in the reactor was controlled at 66 cm^3 (STP)/min.

The final gas flow after being condensed and dried was analyzed offline in the gas chromatographs (GC522) equipped with a thermal conductivity detector (TCD) and a TDx-01 column for N_2, H_2, CO_2, CO, CH_4 and C_2 (C_2H_2, C_2H_4, C_2H_6), while the condensed liquid was sent to the other gas chromatographs (GC7890II) with a flame ionization detector (FID) and a DB-FFAP column where $C_2H_4O_2$, C_3H_6O and C_2H_2O can be quantified.

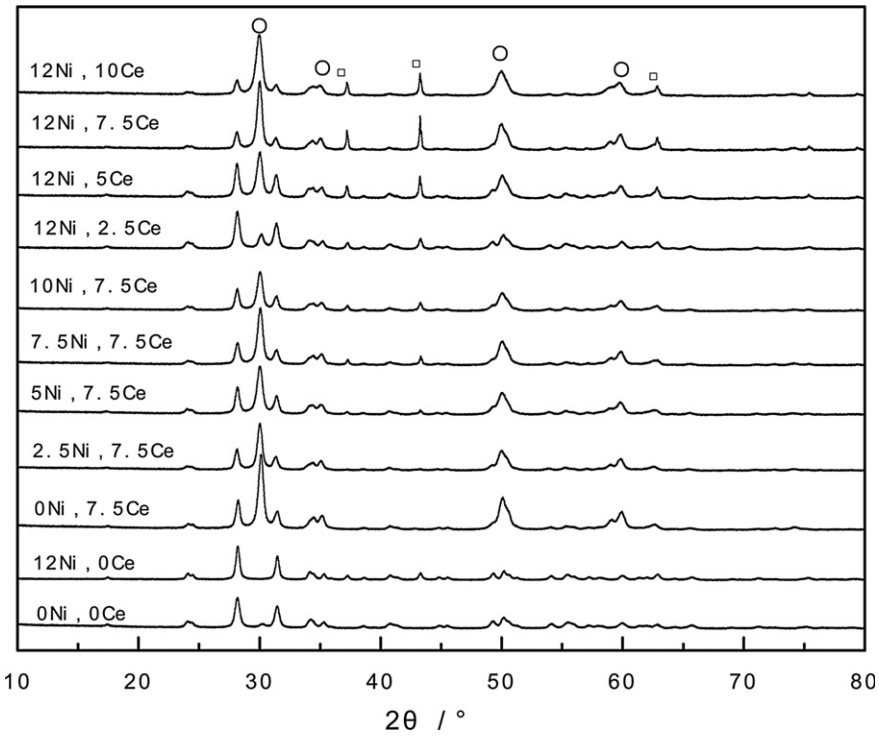

Fig. 1 – XRD patterns for the catalysts Ni/Ce–Zr–O with different Ni and Ce loading: (□) NiO rhombohedral phase; (○) $Ce_{0.1}Zr_{0.9}O_2$ tetragonal phase.

2.4. *Data analysis*

The acetic acid steam reforming performance over Ni catalyst supported on ceria–zirconias was studied by measuring the percent conversion of acetic acid and the selectivity of H_2, CO, CO_2 and CH_4. The expressions are by following.

$$V(H_2)\% = \text{the measured value of } H_2 \text{ volume fraction} / \text{the measured value of } V(H_2+CO+CO_2+CH_4)\% \times 100\% \quad (1)$$

CO, CO_2 and CH_4 are the same as H_2

$$C_A\% = (\text{moles of HAc in the feed} - \text{moles of HAc in the effluent}) / \text{moles of HAc in the feed} \times 100\% \quad (2)$$

$$S(H_2)\% = \text{moles of } H_2 \text{ obtained} / (4 \times (\text{moles of HAc in the feed} - \text{moles of HAc in the effluent})) \times 100\% \quad (3)$$

$$S(C)\% = \text{moles of C obtained} / (2 \times (\text{moles of HAc in the feed} - \text{moles of HAc in the effluent})) \times 100\% \quad (4)$$

$C = CO,\ CH_4,\ CO_2$

3. Results and discussions

3.1. *Catalyst characterizations*

The results of BET and XRD for the Ni/Ce–Zr–O catalysts are shown in Table 1 and Fig. 1, respectively. When the loading of Ce increases from 0 to 7.5%, the BET surface area increases from 8.96 $m^2\ g^{-1}$ to 14.61 $m^2\ g^{-1}$. It was found that, after adding Ce into the catalyst, the XRD patterns of $Ce_{0.1}Zr_{0.9}O_2$ show visible tailing at about 30.0°, 34.9°, 49.8° and 59.6°, (2θ) which represent the indices of (1,0,1), (1,1,0), (1,1,2) and (2,1,1) planes, respectively. This indicates a tetragonal structure, which has a greater oxygen storage space than ZrO_2 monoclinic structure. However, the surface area decreases with the further increase of Ce content to 10 wt%. Combined to XRD, the NiO peak is much stronger at Ce content being 7.5%. The probably reason is that the moderate Ce can interact with Ni and form highly dispersed Ni, increasing the number of

Table 1 – BET surface areas (m^2/g) of catalysts.

Catalysts Ni/Ce–Zr–O		BET surface areas/$m^2\ g^{-1}$
Ni/wt%	Ce/wt%	
12	0	8.96
12	2.5	9.56
12	5	12.04
12	10	11.41
12	7.5	14.61
10	7.5	16.28
7.5	7.5	18.55
5	7.5	20.36
2.5	7.5	25.34
0	7.5	44.11
0	0	47.33

active atom and further improving the activity of catalyst. Meanwhile, it is found that the BET surface area of the carrier ceria–zirconias solid solution is higher than that of adding Ni catalysts. As more content of Ni is loaded, the BET surface area becomes smaller. Corresponding to the XRD, with the content of Ni increasing, the peak of NiO becomes sharp and narrow, implying that the active metal has a low dispersion on the carrier, which results in the reduction of BET surface areas.

3.2. *Influence of reaction temperature*

The reaction temperatures ranging from 500 °C to 900 °C were investigated on the acetic acid steam reforming over 12Ni/7.5Ce-Zr-O at steam to carbon ratio (S/C) of 3 and liquid hourly space velocity (LHSV) of 4.2 h^{-1}. The result shows that when the temperature is higher than 500 °C, the conversion of acetic acid approaches to 100%. Fig. 2 presents that the reaction temperature has significant effects on the selectivity of gaseous products. When the selectivity of CO reaches the maximum value, CO_2 arrives at the minimum value at 900 °C. This possibly because the water gas shift reaction (WGS: $CO + H_2O \rightarrow CO_2 + H_2$) is endothermic reaction and it is not favored at high temperature, as a result, the reverse water gas shift reaction and the thermal decomposition reaction mainly occurred. Under the lower temperature (500 °C–750 °C), hydrogen selectivity varies a little differently with the temperature change. The hydrogen selectivity goes up from 500 °C to 650 °C, then keeps constant until 750 °C, and then goes down after 750 °C. Meanwhile, CH_4 content keeps decreasing from 500 °C to 750 °C. Nevertheless the selectivity of hydrogen decrease obviously accompanied by the rapid increase of the CO content when the reaction temperature reaches 900 °C. The possible reason is that the decomposition of acetic acid is the major pathway at such a high temperature as it shows the largest change in Gibbs energy. That is, it is that the decomposition other than the reforming of acetic acid could occur at the very high temperature.

3.3. *Influence of LHSV*

Different molecules are activated by the catalyst in different ways, which finally results in the different reaction rate. Therefore, the effect of liquid hourly space velocity (LHSV) on catalytic performance was investigated over the 12Ni/7.5Ce-Zr-O catalyst at $T = 650$ °C, $S/C = 3$ and the results are summarized in Fig. 3. With LHSV increased from 2.8 to 4.2 h^{-1}, the selectivity of CO_2 first rises up to 73.3% and then decreases, while the selectivity of H_2 keeps decreasing. Combined with the change trend of CH_4 selectivity which turns out to be contrary to that of hydrogen, we can infer that with LHSV increase, less methane molecules as well as steam molecules are activated to be reformed while much more acetic acid molecules are activated to be thermally decomposed as CH_4 and CO_2. Besides, the space velocity greater than 9 h^{-1} affects the conversion of acetic acid significantly, as is shown in Fig. 3. With LHSV increasing, the conversion of acetic acid decreased from 100% to 89.9%, because of less acetic acid molecules more difficultly being activated in shorter residence time. Therefore, acetic acid molecular is much easier to be activated than methane molecular and steam molecular in a short time, which indicates that the lower LHSV is more conducive for the water gas shift reaction.

3.4. *Influence of steam to carbon ratio*

Steam to carbon ratio plays an important role in the reforming reaction. The performance of the steam reforming of acetic acid on the 12Ni/7.5Ce-Zr-O with the S/C range of 0–3.5 at $T = 650$ °C and LHSV = 2.8 h^{-1} is shown in Fig. 4. With S/C increasing from 0 to 3, hydrogen selectivity increased from 32.5% to 83.4%, and CO content and CH_4 content decreased

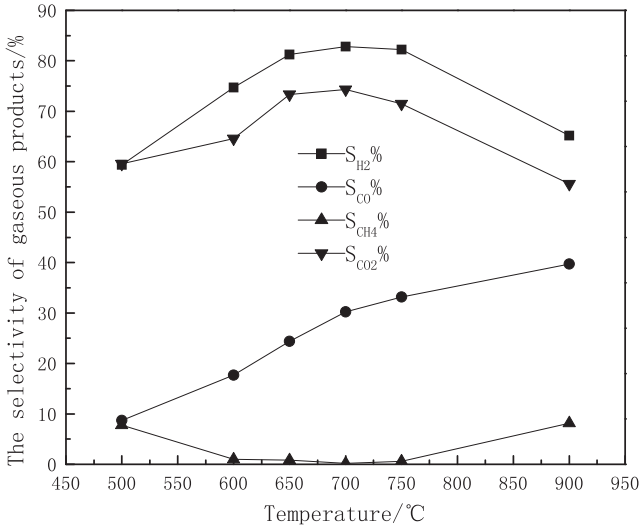

Fig. 2 – Effect of reaction temperature on the selectivities of gaseous products: S/C = 3, LHSV = 4.2 h^{-1}.

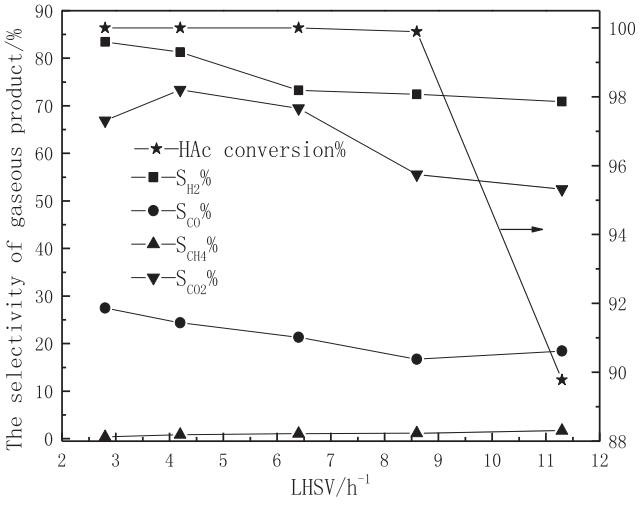

Fig. 3 – Effect of LHSV on the selectivities of gaseous products and the conversion of acetic acid: S/C = 3, T = 650 °C.

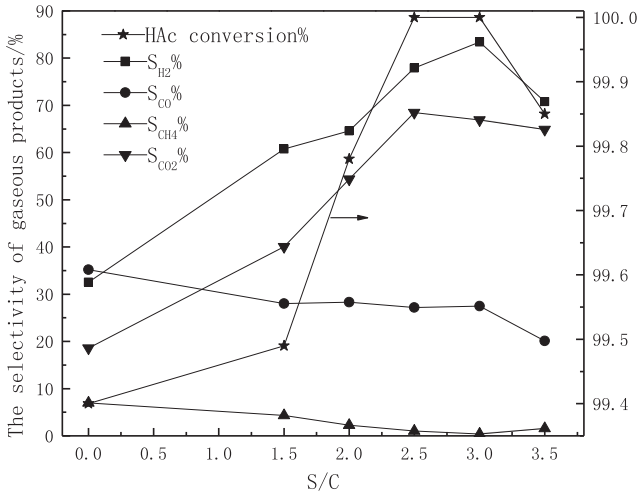

Fig. 4 – Effect of steam to carbon ratio on the selectivities of gaseous products and the conversion of acetic acid: $T = 650\ ^{\circ}C$, LHSV = 2.8 h^{-1}.

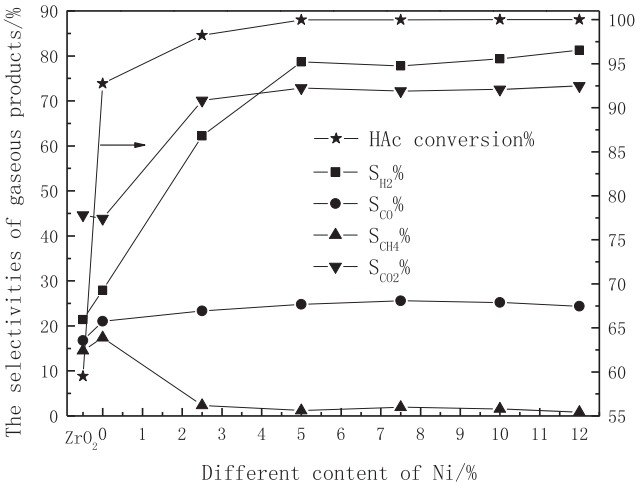

Fig. 5 – Effect of the content of Ni on the selectivities of gaseous products and the conversion of acetic acid: S/C = 3, LHSV = 4.2 h^{-1}.

instead, which indicated that the higher S/C ratio promotes not only the water gas shift reaction (WGS: $CO + H_2O \rightarrow CO_2 + H_2$) but also the methane reforming reaction ($CH_4 + 2H_2O \rightarrow CO_2 + 4H_2$) to the positive direction and that the production of hydrogen is improved significantly, which is consistent with the equilibrium chemical kinetics. Nevertheless, when the water concentration keeps going up, all the results appeared a phenomenon of decline other than CH_4. From Fig. 4, as the S/C ratio reaches 3.5, hydrogen selectivity shows a declining tendency because the activation of steam molecular costs longer time than the activation of acetic acid molecular, which leads to less acetic acid molecular being activated to participate in the reaction and as a result, lead to a lower conversion of acetic acid to H_2, and less CH_4 being reformed. An interesting phenomenon is that when there is no water accompanying acetic acid (S/C = 0) as reactants, acetic acid still can be conversed and its conversion rate reaches 99.4%. Simultaneously, the selectivity of H_2, CO, CH_4, CO_2 are 32.5%, 35.2%, 7.0%, 18.6%, respectively, which indicates that the Ni catalyst supported on ceria–zirconia can promote acetic acid being thermally decomposed mainly into H_2, CO, CH_4, CO_2.

3.5. *Influence of Ni loading*

As the active component, the content of Ni directly influences the catalyst activity and hydrogen yield to some extent. In order to investigate the influence of Ni content on the steam reforming reaction of acetic acid, the reaction conditions are shown in Fig. 5 as the following: the Ce content of 7.5 percent by weight, reaction temperature of 650 °C, steam to carbon molar ratio of 3 and the liquid hourly space velocity of 4.2 h^{-1}. In Fig. 5, when there is no Ni in the catalyst, the conversion of HAc is about 92.8% and the selectivity of CO_2 is obviously higher than that of H_2, moreover, the selectivity of CH_4 stays in a higher level, which indicates that the catalyst ceria–zirconias solid solution can promote the cracking of C–C bond. Note that when the catalyst contains only ZrO_2, the conversion of acetic acid is about 59.5%, but as the promoter Ce being added, the conversion of acetic acid is obviously improved, which indicates that the promoter Ce can promotes the cracking of C–C bond. However, with the content of Ni being added in, the conversion of HAc and the selectivity of hydrogen both significantly increases: the former increases from 92.8% to 100% and the latter increases from 78.9% to 81.3%, simultaneously, the selectivity of CH_4 decreases from 18% to 0.4%, which indicated that the active component Ni promotes not only the cracking of C–C bond but also the cracking of C–H bond.

3.6. *Influence of Ce loading*

As we have mentioned, CeO_2 is chosen as a promoter because it is an important material for a variety of catalytic reaction involving oxidation and reforming of hydrocarbons. In this part, steam reforming of acetic acid was carried out at the Ni catalyst supported on ceria–zirconias with the Ce content of 0, 2.5%, 5%, 7.5% and 10% by weight respectively under the reaction temperature of 650 °C, the steam to carbon ratio of 3 and LHSV of 4.2 h^{-1}. Fig. 6 shows clearly that there is the growth of the conversion of acetic acid as the promoter Ce is added. Combined with XRD in Fig. 1 and BET in Table 1, we can see that proper content of Ce being added in the catalyst promotes the dispersion of the active component Ni and improves the BET surface area of the catalyst. When the content of Ce is added to 7.5%, the maximum selectivity of both H_2 and CO_2 are obtained due to the enhancement of water adsorption/dissociation on the Ni–Ce interfaces developed on the catalyst resulting in Ce-promoted catalysts the improvement in intrinsic activity [27]. It is noticeable that when added the active component Ni into the support ZrO_2 (without the promoter Ce), the conversion of acetic acid and the selectivity of hydrogen both improved greatly, which is consistent with the result of 3.5.

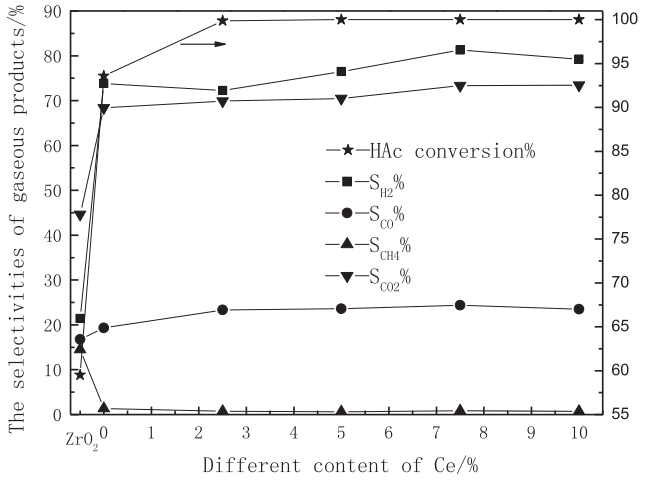

Fig. 6 – Effect of the content of Ce on the selectivities of gaseous products and the conversion of acetic acid: T = 650 °C, S/C = 3, LHSV = 4.2 h^{-1}.

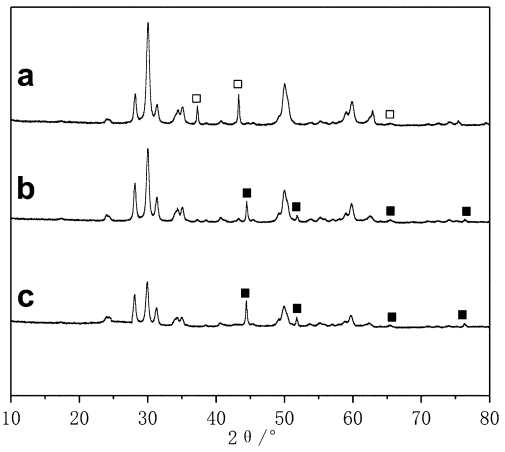

Fig. 8 – XRD patterns for the 12Ni/7.5Ce-Zr-O catalysts: (a) before reduction and (b) after reduction (c) after reaction (□) NiO rhombohedral phase; (■) Ni cubic phase.

3.7. *The stability of Ni catalyst supported on ceria–zirconia*

Taking into account that Ni catalyst supported on ceria–zirconia showed the best performances at $T = 650$ °C, $S/C = 3$, stability test was carried out under the same condition to better insight its catalytic behaviors. The test continued for 25 h and the results were shown in Fig. 7. It could be seen that Ni catalyst supported on ceria–zirconia maintained its activity and selectivity for all the time-on-stream under the reaction conditions. During the reaction, the condensed acetic acid liquid wasn't detected by a DB-FFAP column in a flame ionization detector (FID). That is, acetic acid can be considered to be completely transformed. Besides, selectivities toward H_2 and CO_2 are high and stable, which can be proved by XRD. As is shown in Fig. 8, the catalysts before and after reaction exhibited the comparable diffraction patterns. For the one before reaction (a), the diffraction peaks centered at $2\theta = 37.3°$, 43.3°and 62.9°, indicated the characteristics of NiO phase. For the one after reaction, there are still the appearances of the characteristic peaks of Ni. The mainly change is the position for the diffraction peak of Ni (44.5°, 51.8°, 62.9°, 76.3°). It can be obtained that little structure change of the catalyst occurs and catalyst still performs higher activity during the 25-h-reaction.

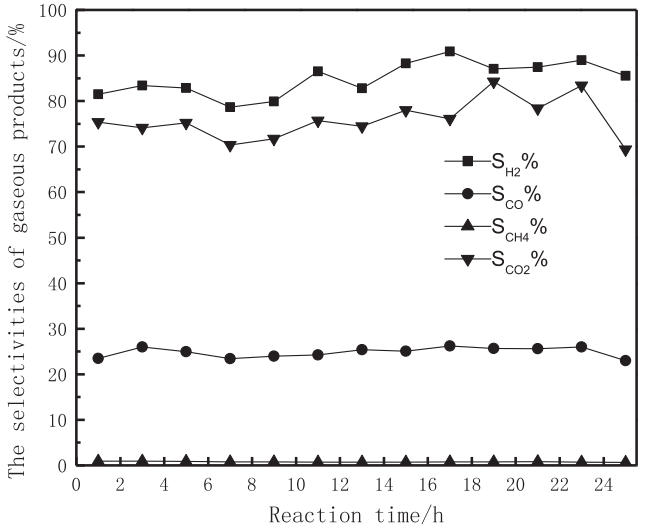

Fig. 7 – The selectivities of gaseous products change with reaction time: T = 650 °C, S/C = 3, LHSV = 4.2 h^{-1}.

4. Conclusions

Acetic acid can be effectively reformed over 12Ni/7.5Ce-Zr-O catalyst with high selectivities toward both H_2 and CO_2. The active component Ni mainly promotes the cracking of C–C bond and C–H bond while the promoter Ce promotes the cracking of C–C bond and dispersion of Ni on the support. This indicates that 12Ni/7.5Ce-Zr-O mainly devotes to the water gas shift reaction. Besides, the optimum conditions are obtained according to the selectivity of hydrogen. Under the reaction temperature of 650 °C, the steam to carbon ratio of 3 and the liquid hourly space velocity of 2.8 h^{-1}, the maximum selectivity of hydrogen 83.4% as well as the minimum methane selectivity 0.39% can be obtained. The catalyst 12Ni/7.5Ce-Zr-O also performs good stability for continuous 25 h-reaction without any deactivation.

Acknowledgments

The authors are grateful for the Natural Science Foundation of China (20806082) and (50306026), and the National Natural Science Foundation of Guangdong province (10151007 006000016).

REFERENCES

[1] Li WP, Wang SD. Methanol steam reforming in a compact plate-fin reformer for fuel-cell systems. Int J Hydrogen Energy 2005;30:973–9.

[2] Yan CF, Hu EY, Cai CL. Hydrogen production from bio-oil aqueous fraction with in situ carbon dioxide capture. Int J Hydrogen Energy 2010;35:2612–6.

[3] Wu SF, Wang LL. Improvement of the stability of a ZrO_2-modified Ni–nano-CaO sorption complex catalyst for ReSER hydrogen production. Int J Hydrogen Energy 2010;35:6518–24.

[4] Furusawa T, Sato T, Sugito H, Miura Y. Hydrogen production from the gasification of lignin with nickel catalysts in supercritical water. Int J Hydrogen Energy 2007;32:699–704.

[5] Hulteberg PC, Karlsson HT. A study of combined biomass gasification and electrolysis for hydrogen production. Int J Hydrogen Energy 2009;34:772–82.

[6] Demirbas A. Characterization of products from two lignite samples by supercritical fluid extraction. Energy Source A 2004;26:933–9.

[7] Therdthianwong S, Srisiriwat N, Therdthianwong A, Croiset E. Reforming of bioethanol over Ni/Al(2)O(3) and Ni/CeZrO(2)/Al(2)O(3) catalysts in supercritical water for hydrogen production. Int J Hydrogen Energy 2009;36:2877–86.

[8] Hu X, Lu GX. Investigation of the steam reforming of a series of model compounds derived from bio-oil for hydrogen production. J Appl Catal B 2009;88:376–85.

[9] Hou T, Yuan LX, Ye TQ, Gong L. Hydrogen production by low-temperature reforming of organic compounds in bio-oil over a CNT-promoting Ni catalyst. Int J Hydrogen Energy 2009;34:9095–107.

[10] Vagia EC, Lemonidou AA. Thermodynamic analysis of hydrogen production via steam reforming of selected components of aqueous bio-oil fraction. Int J Hydrogen Energy 2007;32:212–23.

[11] Wang D, Montane D, Chornet E. Catalytic steam reforming of biomass-derived oxygenates: acetic acid and hydroxyacetaldehyde. Appl Catal A 1996;143:245–70.

[12] Zhang SP, Li XJ, Li QY, Xu QL, Yan YJ. Hydrogen production from the aqueous phase derived from fast pyrolysis of biomass. J Anal Appl Pyrolysis 2011;92:158–63.

[13] Kan T, Xiong JX, Li XL, Ye TQ, Yuan LX, Torimoto Y, et al. High efficient production of hydrogen from crude bio-oil via an integrative process between gasification and current-enhanced catalytic steam reforming. Int J Hydrogen Energy 2010;35:518–32.

[14] Wu C, Liu RH. Carbon deposition behavior in steam reforming of bio-oil model compound for hydrogen production. Int J Hydrogen Energy 2010;35:7386–98.

[15] Iwasa N, Yamane T, Takei M, Ozaki JI, Arai M. Hydrogen production by steam reforming of acetic acid: comparison of conventional supported metal catalysts and metal-incorporated mesoporous smectite-like catalysts. Int J Hydrogen Energy 2010;35:110–7.

[16] Lulianelli A, Longo T, Basile A. CO-free hydrogen production by steam reforming of acetic acid carried out in a Pd–Ag membrane reactor: the effect of co-current and counter-current mode. Int J Hydrogen Energy 2008;33:4091–6.

[17] Basagiannis AC, Verykios XE. Catalytic steam reforming of acetic acid for hydrogen production. Int J Hydrogen Energy 2007;32:3343–55.

[18] Basagiannis AC, Verykios XE. Reforming reactions of acetic acid on nickel catalysts over a wide temperature range. Appl Catal A 2006;308:182–93.

[19] Rioche C, Kulkarni S, Meunier FC, Breen JP, Burch R. Steam reforming of model compounds and fast pyrolysis bio-oil on supported noble metal catalysts. Appl Catal B 2005;61:130–9.

[20] Rajadurai S. Pathways for carboxylic-acid decomposition on transition-metal oxides. Catal Reviews-Science Eng 1994;36:385–403.

[21] Pestman R, Koster RM, vanDuijne A, Pieterse JAZ, Ponec V. Reactions of carboxylic acids on oxides .2. Bimolecular reaction of aliphatic acids to ketones. J Catal 1997;168:265–72.

[22] Roh HS, Jun KW, Dong WS, Chang JS, Park SE, Joe YI. Highly active and stable Ni/Ce–ZrO_2 catalyst for H_2 production from methane. J Mol Catal A-Chemical 2002;181:137–42.

[23] Biswas P, Kunzru D. Steam reforming of ethanol for production of hydrogen over Ni/CeO_2–ZrO_2 catalyst: effect of support and metal loading. Int J Hydrogen Energy 2007;32:969–80.

[24] Li SR, Li MS, Zhang CX, Wang SP, Ma XB, Gong JL. Steam reforming of ethanol over Ni/ZrO_2 catalysts: effect of support on product distribution. Int J Hydrogen Energy 2012;37:2940–9.

[25] Vagia EC, Lemonidou AA. Investigations on the properties of ceria–zirconia-supported Ni and Rh catalysts and their performance in acetic acid steam reforming. J Catal 2010;269:388–96.

[26] Yan CF, Cheng FF, Hu RR. Hydrogen production from catalytic steam reforming of bio-oil aqueous fraction over Ni/CeO_2–ZrO_2 catalysts. Int J Hydrogen Energy 2010;35:11693–9.

[27] Sanchez MC, Navarro RM, Fierro JLG. Ethanol steam reforming over Ni/M_xO_y-Al_2O_3 (M = Ce, La, Zr, and Mg) catalysts: influence of support on the hydrogen production. Int J Hydrogen Energy 2006;32:1462–71.